Signal Processing ▮ (▮▮▮▮) ▮▮▮–▮▮▮

Contents lists available at ScienceDirect

Signal Processing

journal homepage: www.elsevier.com/locate/sigpro

Cognitive OFDM system detection using pilot tones second and third-order cyclostationarity ☆

François-Xavier Socheleau [a,*], Sébastien Houcke [a], Philippe Ciblat [b], Abdeldjalil Aïssa-El-Bey [a]

[a] Institut TELECOM; TELECOM Bretagne; UMR CNRS 3192 Lab-STICC, Université européenne de Bretagne, Technopôle Brest Iroise-CS 83818, 29238 Brest Cedex, France

[b] Institut TELECOM; TELECOM ParisTech, 46 rue Barrault, 75013 Paris, France

ARTICLE INFO

Article history:
Received 23 November 2009
Received in revised form
29 March 2010
Accepted 7 July 2010

Keywords:
Cognitive radio
Vertical handoff
Detection
OFDM
Pilot tones
Cyclostationarity
m-Sequence

ABSTRACT

The emerging trend to provide users with ubiquitous seamless wireless access leads to the development of multi-mode terminals able to smartly switch between heterogeneous wireless networks. This switching process known as vertical handoff requires the terminal to first detect the surrounding networks it is compatible with. In the context where these networks are cognitive, this can be challenging since the carrier frequency of their access point may change over the time. One solution to overcome this challenge is to embed network specific signatures in the PHY layer. We here focus on cognitive OFDM systems and advocate to embed signatures onto pilot tones since (i) it makes possible to discriminate systems with the same modulation parameters (ii) it creates easy to intercept signatures implying short detection latency (iii) it avoids adding any side information dedicated to detection that would reduce systems capacity. We propose two complementary signature/detection schemes based on second and third-order statistics, respectively. The first scheme relies on redundancy between pilot symbols and the second is based on the use of maximum-length sequences. Detailed numerical examples demonstrate the efficiency of the two detection criteria in realistic environments.

1. Introduction

To accommodate the anticipated growth in mobile services, there is ongoing pressure on regulators to make additional spectrum available for mobile applications. As a consequence of the physical limits on the amount of available spectrum, regulatory policies are evolving in the some bands from the current fixed spectrum rules to opportunistic spectrum sharing models [3,4]. These new policies open up the possibility to make a clever use of the radio resources by developing devices embedding cognitive radio (CR) technologies [5,6]. CR enables dynamic spectrum access [7] by sensing the electro-magnetic environment and specifically by detecting and then operating on idle frequency channels (known as white spaces) at a particular time and place [6]. From a service provider perspective, CR can improve the spectral efficiency [8] and therefore increase the capacity.

In parallel to the development of new mobile services, there is an emerging trend to provide users with ubiquitous seamless wireless access. This can be made possible by taking advantage of the coexistence of complementary heterogeneous networks. In such environment, a challenge is to develop multi-mode terminals (relying on software radio technologies [9]) able to

☆ This material is based upon work supported by Agence Nationale de la Recherche under grant "DEMAIN". Part of this work was presented at IEEE PIMRC 2008 [1] and IEEE WCNC 2009 [2].

* Corresponding author.
E-mail addresses: fx.socheleau@telecom-bretagne.eu (F.-X. Socheleau), sebastien.houcke@telecom-bretagne.eu (S. Houcke), philippe.ciblat@telecom-paristech.fr (P. Ciblat), abdeldjalil.aissaelbey@telecom-bretagne.eu (A. Aïssa-El-Bey).

0165-1684/$ - see front matter © 2010 Elsevier B.V. All rights reserved.
doi:10.1016/j.sigpro.2010.07.003

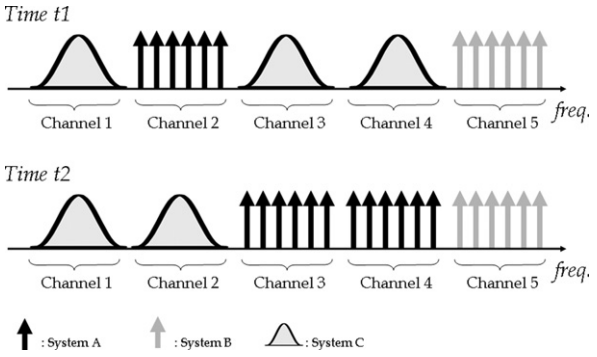

Fig. 1. Example of a channel occupation scenario where three systems share the same frequency range divided into 5 channels. Note that these channels may not be contiguous.

smartly switch from one wireless interface to another while maintaining IP or voice connectivity and required QoS. This switching process is known as "vertical handoff". In contrast with horizontal handoff (handoff within a network made of homogeneous wireless interfaces), vertical handoff triggering is based on a multi-criteria decision involving signal quality, bandwidth, traffic load, price, battery status, latency, etc. [10,11]. Before measuring any of these metrics relevant to trigger a potential handoff, the first task to be executed by a multi-mode terminal is to detect the surrounding wireless networks it is compatible with.[1]

In the classical framework of static frequency allocation policies, the terminal knows the carrier frequency values of the networks of interest. Network access points (AP) detection can thus easily be performed using energy detectors or filters matched to downlink frame preambles. In a cognitive context, AP's carrier frequency may change over the time since the spectrum availability depends on interaction between systems sharing the same band (see Fig. 1). Therefore, if we assume that the spectrum is divided into a finite number of frequency channels, the number and the frequency of the channels used by a given cognitive AP may not be a priori known by the multi-mode terminal. This situation prevents from using energy detectors but still allow the use of matched filters. As a reference, for initial detection/synchronization in a cognitive context, the IEEE 802.22 working group [12] has defined a superframe structure that encapsulates classical frames and that starts with a preamble duplicated on every channel used by an AP. When sensing all the potential active channels, if a terminal finds a superframe header on a particular frequency channel it then obtains all the necessary information (number and frequency of all the channels used by the AP, etc.) to demodulate the frames that follow [13]. This mechanism is pretty efficient as the channel detection can be performed by simple cross-correlation between the received signal and the known preamble sequence. In addition, a terminal only needs to detect a single channel to gather all the information to get connected to the network. However, the drawback of the superframe is that it decreases the network capacity so that the superframe header must not be sent frequently to limit the overhead. As an example, the 802.22 superframe header is only broadcasted every 160 ms which corresponds to 16 frames. In our context where a multi-mode terminal is sensing several networks of interest, it may not tolerate a too long latency in detecting all APs before deciding which one is the most suited to its needs. For each AP to be detected, the matched filter approach can indeed be a very long process if the set of possible active channels is large. For instance, in the worse case scenario, 802.22 matched filter detection can take up to 10 s as there can be more than 60 potential active channels [13].

To limit the handoff latency resulting from matched filter detection, an alternative approach consists in embedding network specific patterns or signatures in the physical signal that are broadcasted at all time. Pattern detection can then be performed at any time by the multi-mode terminal to identify spectrum bands in use by the cognitive networks of interest. More generally, the set of minimum requirements that a signature scheme and its associated detectors must meet is[2]:

- Cognitive systems operating in the same frequency bands must be discriminable. This requires to design signature schemes that can generate as many patterns as operating networks as well as detectors that guarantee a low false alarm rate.
- System signatures must be quickly detectable. Parallel sensing of all channels may not be always feasible, specifically in the scenario where the frequency range of the possible active channels is wider than the receiver RF bandwidth of the receiver (see the IEEE 802.22 standard [12] for instance). In that case, to avoid long connection latencies, the sensing period of each channel must be short. This means that signatures must be broadcasted at all time and that detection must be effective with small portions of signal.
- The signature scheme must not decrease the system capacity. Signaling overhead must be prohibited to avoid any bandwidth loss.

In contrast with licensed user detection [14], cognitive system detection at negative SNR is not required here. Detectors must only guarantee good performance in SNR ranges where systems experience bit error rates low enough to operate. Detection as such is not much of interest if the vertical handoff cannot be triggered afterward due to a poor signal quality.

In this paper we focus on OFDM based systems as it is a good physical layer candidate for cognitive systems since it is scalable by turning on or off some subcarriers and eases spectrum sensing in the frequency domain thanks to its built-in FFT [15]. Obvious OFDM signatures can be created

[1] In the remainder of the paper, these wireless networks are mentioned as "networks of interest".

[2] These requirements are deliberately qualitative to be independent of a specific context.

Please cite this article as: F.-X. Socheleau, et al., Cognitive OFDM system detection using pilot tones second and third-order cyclostationarity, Signal Process. (2010), doi:10.1016/j.sigpro.2010.07.003

thanks to the cyclic prefix (CP) as its duration and periodicity could be system specific. That is why OFDM detection has mainly been studied using various correlation or cyclostationary properties induced by the CP [16–20]. However, the performance of this approach is drastically dependent on the cyclic prefix duration and can be affected by multipath propagation channels. Moreover, such method is totally inefficient in the presence of a zero-padded OFDM system which may be relevant in a cognitive context [21]. In addition, in a CR scenario, it is very likely that OFDM systems competing for the access to the same frequency band will have the same (or very close) modulation parameters (subcarrier spacing, CP length, etc.). The PHY layer design is indeed strongly driven by features related to the spectrum in which a system operate (propagation channel, available bandwidth, etc.). Therefore, methods that involve more particular signatures in cognitive OFDM systems may be required and very useful.

In [22,23], the authors suggest approaches using dedicated subcarriers with cyclostationary patterns. However, dedicating subcarriers to only embed signatures may have a cost as it adds overhead and thus reduces networks capacity. One way to address this issue is to merge subcarriers used for system detection with existing pilot tones typically applied in wireless systems. Pilot tones are of great interest since they are (almost) always present in the transmitted signals and therefore easy to intercept and avoid adding any signaling overhead dedicated to detection purposes. Existing pilot tones are mainly designed for channel estimation [24], synchronization [25] and/or to carry system control information (or signaling) [26–28].

Therefore, adding a new purpose to pilot subcarriers (for instance, system detection) requires dealing with some already existing constraints, hereafter itemized into two categories:

1. Time–frequency pilot tones distribution—signature patterns cannot impose a specific pilot tone arrangement in the time–frequency plane as it is usually driven by channel estimation requirements [29].
2. Pilot sequences carrying signaling information—this second constraint, usually added on top of the first one, only affects systems that transmit protocol signaling through pilot tones. In this case, pilots embed sequences belonging to a finite set of codewords known at reception which are decoded by simple cross-correlation (e.g. [27,28]). In this context, pilot sequences have to verify low cross-correlation properties to avoid wrong decoding at reception.

In this contribution, we analyze two solutions to embed detection signatures onto pilot tones of OFDM signals without decreasing networks capacity. In both cases, signature detection is robust to the channel as well as to synchronization impairments. This detection is only based upon the knowledge of pilot structures without knowledge of pilot symbols so that, in contrast with coherent detection, it can be performed on every portion of the received signal. The first approach induces correlation between pilot subcarriers and exploits the deterministic and periodic characteristics of pilot mapping in the time–frequency domain. For this method, system signatures and their associated detectors are thus based on second-order cyclostationary properties. The second approach considers systems using pilots to carry protocol signaling and relies on the use of maximum-length sequence also known as *m*-sequence. Thanks to their low correlation properties, *m*-sequences are good candidates for standard signaling. We also demonstrate that such sequences show higher-order properties relevant to distinguish systems from each other and therefore advocate to generalize their use in a cognitive context.

The paper is organized as follows: Section 2 describes the signal pre-processing implemented in the terminal front-end prior to detection and also presents the OFDM system model. Section 3 recalls the cyclostationarity basis and introduces a novel second-order pilot-induced cyclostationary (PIC) signature scheme with its corresponding detector. In Section 4, *m*-sequences properties are detailed, a *m*-sequence (MS) signature scheme is proposed, and the associated detection cost function is derived. Detection performance is assessed through simulations in Section 5. Finally, conclusions are presented in Section 6.

2. Signal pre-processing and OFDM system model

2.1. Signal pre-processing

The current design of multi-mode terminals is based on software defined radio technology that enables through software, dynamic reconfiguration of all protocol stacks including the physical layer [30]. A basic front-end of a software radio is made of a RF module, an IF downconverter and a ADC followed by a digital front-end. This digital front-end embeds downconverters, filters and sample-rate converters, that adapt the bandwidth and the sampling frequency of the acquired signal to match the PHY features of the air-interface to be processed [31]. Multi-mode terminals thus have the ability to perform multirate signal processing. The output of the digital front-end is then fed into the baseband processing engine that detects, demodulates, decodes, etc. the signal. Note that a baseband processing engine can service multiple RF front-ends, each of which supports specific air interface standards operating in a specific frequency band of interest [9]. In this paper, we limit the scope of the baseband processing engine to detection. Fig. 2 represents the functional diagram of a multi-mode terminal in a scenario where it senses a frequency channel in which three different OFDM cognitive networks of interest can potentially operate. Since these networks may have different modulation parameters, upon signal acquisition, the digital front-end provides three output signals, each of which is tailored to the PHY features of a particular network. Typically, signal A (resp. B and C) has a sampling frequency that is a multiple of the subcarrier spacing of system A (resp. B and C). These three signals are then sent to the detector that makes a decision on the presence or absence of these systems in the sensed frequency channel.

Please cite this article as: F.-X. Socheleau, et al., Cognitive OFDM system detection using pilot tones second and third-order cyclostationarity, Signal Process. (2010), doi:10.1016/j.sigpro.2010.07.003

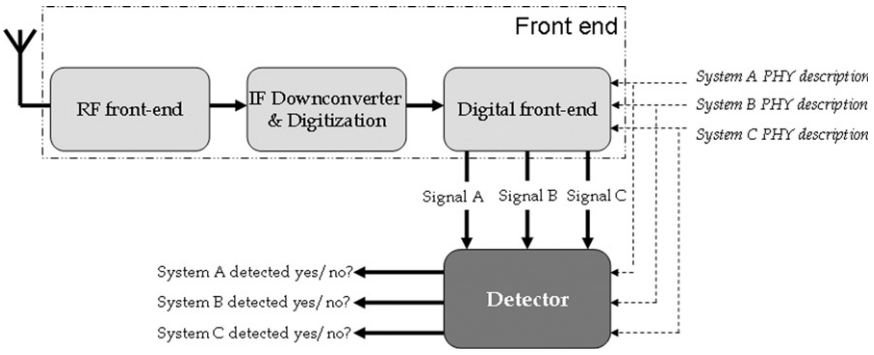

Fig. 2. Block diagram of the multi-mode terminal.

2.2. Pilot-assisted OFDM system model

Assuming that in a given frequency channel, a transmitted OFDM symbol consists of N subcarriers, the discrete-time baseband equivalent transmitted signal is given by

$$x(m)=\sqrt{\frac{E_s}{N}}[x_d(m)+x_t(m)], \tag{1}$$

where

$$x_d(m)=\sum_{k\in\mathbb{Z}}\sum_{\substack{n=0\\ n\notin\mathcal{I}(k)}}^{N-1} a_k(n)e^{2i\pi(n/N)(m-D-k(N+D))}g(m-k(N+D))$$

and

$$x_t(m)=\sum_{k\in\mathbb{Z}}\sum_{n\in\mathcal{I}(k)} b_k(n)e^{2i\pi(n/N)(m-D-k(N+D))}g(m-k(N+D)). \tag{2}$$

E_s is the signal power and $a_k(n)$ are the transmitted data symbols at n-th subcarrier of k-th OFDM block. These data symbols are assumed to be independent and identically distributed (i.i.d.), D is the CP length; $m\mapsto g(m)$ is the pulse shaping filter. $\mathcal{I}(k)$ denotes the set of pilot subcarrier indexes of the k-th symbol and $b_k(n)$ are the pilot symbols.

Let $\{h(l)\}_{l=0,\ldots,\ L-1}$ be the baseband equivalent discrete-time channel impulse response of length L. Unless otherwise stated, the channel is assumed to be time invariant. Notice that the impact of channel variations is discussed in Section 5. At the output of the digital front-end, the samples of the OFDM signal are then expressed as

$$y(m)=e^{-i(2\pi\varepsilon(m-\tau)/N+\theta)}\sum_{l=0}^{L-1}h(l)x(m-l-\tau)+\eta(m), \tag{3}$$

where ε is the carrier frequency offset (normalized by the subcarrier spacing), θ the initial arbitrary carrier phase, τ the timing offset and $\eta(m)$ a zero mean circularly symmetric complex-valued white Gaussian noise of variance σ^2 per complex dimension.

As depicted in Fig. 3, three different types of pilot tone arrangements are usually set up in OFDM systems to meet the channel estimation constraints. The first one is the block type configuration used under the assumption of slow fading channel. Pilot tones are in that case mapped onto all subcarriers of OFDM symbols within a specific

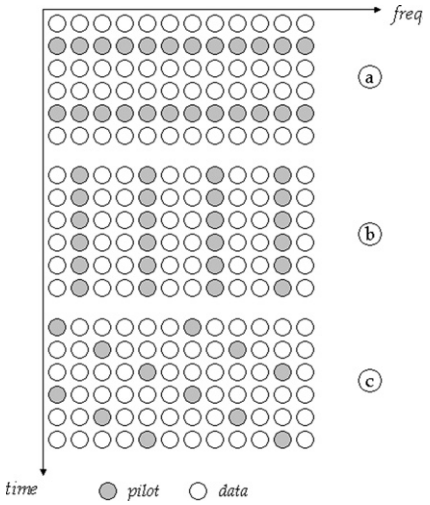

Fig. 3. Examples of pilot tone arrangement: (a) block-type configuration, (b) comb-type configuration, (c) circular configuration.

period K so that $\mathcal{I}(k)$ verifies

$$\mathcal{I}(k)=\begin{cases}\{0,\ldots,\ N-1\} & \text{if } k=mK(m\in\mathbb{Z}),\\ \emptyset & \text{otherwise.}\end{cases}$$

The second one, comb-type pilot configuration, is introduced to satisfy the need for equalizing when the channel quickly varies. Pilot tones are mapped onto certain subcarriers of each OFDM symbol such that $\mathcal{I}(k)=\mathcal{I}$ where $\mathcal{I}$ is any subset of $\{0,\ldots,N-1\}\forall k$. The last arrangement is a circular configuration where the set of pilot subcarrier indexes periodically change such that $\mathcal{I}(k+K)=\mathcal{I}(k)$ where $K\in\mathbb{Z}$ and $\mathcal{I}(k)\neq\emptyset$. Such a scheme is used under the assumption of fast fading channel and presents the interest of avoiding cases where a given pilot subcarrier is attenuated by the channel for a period of several symbols. Note that some OFDM systems (e.g. [32,26]) make a joint use of these arrangements.

3. Second-order pilot-induced cyclostationary signatures

In this section, we propose to induce joint cyclostationarity between pilot tones to create system specific

Please cite this article as: F.-X. Socheleau, et al., Cognitive OFDM system detection using pilot tones second and third-order cyclostationarity, Signal Process. (2010), doi:10.1016/j.sigpro.2010.07.003

signatures. The basics on cyclostationarity are first recall in Section 3.1. We present in Section 3.2 the degrees of freedom that define a second-order pilot-induced cylostationary (PIC) signature. A detector tailored to the proposed signature scheme is then detailed in Section 3.3. To facilitate the derivation and the understanding of the detector, the method is first introduced by assuming perfect synchronization at reception. This assumption, purely didactic, is then relaxed in Section 3.4 in order to make the proposed detector robust to synchronization impairments.

3.1. Background on cyclostationarity

Two complex discrete time stochastic processes x_k and y_k, $k \in \mathbb{Z}$, are said to exhibit joint second-order almost cyclostationarity in the wide sense if the cross-correlation function

$$R_{xy}(k,u) \triangleq \mathbb{E}[x_k y_{k+u}^*],$$

where * stands for complex conjugation, admits a series representation

$$R_{xy}(k,u) = \sum_{\alpha \in \mathcal{A}_{xy}} R_{xy}^{\alpha}(u) e^{i2\pi\alpha k},$$

where

$$R_{xy}^{\alpha}(u) \triangleq \lim_{M \to +\infty} \frac{1}{2M+1} \sum_{k=-M}^{M} R_{xy}(k,u) e^{-i2\pi\alpha k} \tag{4}$$

is the cyclic cross-correlation function (CCCF) and

$$\mathcal{A}_{xy} \triangleq \{\alpha \in [-1/2; 1/2[\mid \exists u \text{ s.t. } R_{xy}^{\alpha}(u) \neq 0\}$$

is a countable set of cycle frequencies α [33]. Note that the CCCF is periodic in α with period 1.

3.2. Pilot-induced cyclostationary (PIC) pattern generation

As illustrated in Section 2.2, the time–frequency pilot tones distribution is always deterministic to meet the channel estimation requirements. For instance, [29] demonstrates that the optimal pilots in the sense of minimizing the channel mean square error (MSE) are those that are equispaced and equipowered. As the number of pilot tones is finite, the deterministic characteristic of the pilot tones distribution can be expressed as $\mathcal{I}(k+K) = \mathcal{I}(k)$, $K \in \mathbb{Z}$ for any combination of arrangements described in Section 2.2. For the particular case of comb-type arrangement, note that $K=1$. Such a periodicity is a useful property that can be exploited to induce cyclostationarity in OFDM frames through careful choice of pilot symbols $b_k(n)$.

Let $c_k(n)$ be the k-th symbol on subcarrier n such that

$$c_k(n) = \begin{cases} b_k(n) & \text{if } n \in \mathcal{I}(k), \\ a_k(n) & \text{otherwise.} \end{cases} \tag{5}$$

Theorem 1. *If the pilot tones are designed such that*

$$b_k(p) = b_{k+d^{(p,q)}}(q) e^{i\varphi}$$

with $d^{(p,q)} \in \mathbb{Z}$ *and* $\varphi \in [-\pi; \pi[$ *then the processes* $\{c_k(p)\}_k$ *and* $\{c_k(q)\}_k$ *are jointly cyclostationary with* $\mathcal{A}_{(p,q)} \triangleq \mathcal{A}_{c_k(p)c_k(q)} = \{(m - \lfloor K/2 \rfloor)/K,\ m \in \{0,1,\ldots,K-1\}\}$ *where* $\lfloor\rfloor$ *stands for integer flooring.*

Proof of Theorem 1 is given in Appendix A.

In the framework of OFDM system detection, joint cyclostationary structure is of great interest to generate system specific signatures. Theorem 1 indicates that it is possible to design a given signature by choosing particular combinations of $p,q,d^{(p,q)}$ and K. For a system with a subcarrier spacing of $1/N$ and a cyclic prefix length of D, such a signature S is then defined as

$$S \triangleq \{(p,q,d^{(p,q)},K) \mid \mathcal{A}_{(p,q)} \neq \emptyset\} \quad \text{given } N \text{ and } D. \tag{6}$$

Fig. 4 shows a schematic illustration of the principle of OFDM joint cyclostationary pattern generation. The signature is $S=\{(0,2,d^{(0,2)}=1,\ K=3),\ (6,7,d^{(6,7)}=-2,\ K=3)\}$, given $N=8$ and any fixed value of D. From Theorem 1, peaks of energy are then obtained for cycle frequencies $\alpha \in \{-\frac{1}{3}, 0, \frac{1}{3}\}$. Note that DVB-T [32], fixed WiMAX [34] or Wifi [35] pilot structures can be seen as (unintentional) PIC signatures.

The signature scheme allows a very large number of possible combinations. However, channel estimation usually requires relatively small K (e.g. $K=4$ for the DVB-T and $K=2$ or 9 for the Mobile WiMAX [26]). In addition, to make the signature usable for detection purposes, $d^{(p,q)}$ has to be upper-bounded by the observation window length necessary to perform the detection (see Section 5). Note also that the term $e^{i\varphi}$ in Theorem 1 is here to bring flexibility to PIC structures and to prevent coherent addition of pilot symbols that would increase the peak-to-average-power ratio (PAPR). This phase shift has no impact on the detection criterion presented in the sequel.

3.3. Pilot-induced cyclostationary pattern detection

3.3.1. Detection cost function

Thanks to Theorem 1, systems satisfying Eq. (1) and (6) have a periodic cross-correlation function $R_{c^{(p,q)}}(k,d^{(p,q)}) = \mathbb{E}[c_k(p) c_{k+d^{(p,q)}}^*(q)]$ and can thus be discriminated by exploiting the cyclic cross-correlation function (CCCF)

$$R_{c^{(p,q)}}^{\alpha}(d^{(p,q)}) \triangleq \lim_{M \to +\infty} \frac{1}{2M+1} \sum_{k=-M}^{M} \mathbb{E}[c_k(p) c_{k+d^{(p,q)}}^*(q)] e^{-i2\pi\alpha k}. \tag{7}$$

We propose to perform the system detection on the evaluation of the CCCF energy at cyclic frequencies $\alpha \in \mathcal{A}_{(p,q)}$. In practice the symbols $c_k(n)$ are only accessible via the observations $Y_k(n)$ expressed as

$$Y_k(n) \triangleq \frac{1}{\sqrt{N}} \sum_{m=0}^{N-1} y[k(N+D)+D+m] e^{-2i\pi nm/N}.$$

In our context, the terminal knows the subcarrier spacing value as well as the cyclic prefix duration of the networks is trying to detect. These values are usually standardized and do not change on the flight. In the case of perfect synchronization (i.e. $\varepsilon = 0$, $\tau = 0$ and $\theta = 0$), the observations simplify to

$$Y_k(n) = H(n) c_k(n) \sqrt{E_s} + \mathfrak{N}_k(n),$$

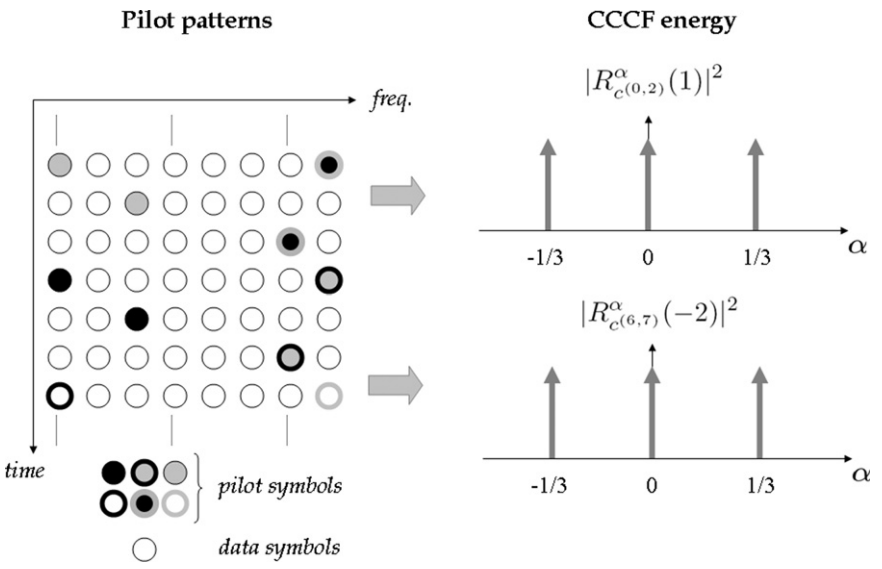

Fig. 4. Schematic illustration of the joint cyclostationary pattern generation. Identical pilot symbols are represented with the same filling colors. The cyclic cross-correlation function (CCCF) is defined in Eq. (7).

where $H(n)$ and $\mathfrak{N}_k(n)$ are, respectively, the channel frequency response at subcarrier n and the noise at subcarrier n of the k-th received symbol. Note that the synchronization impairments are studied in Section 3.4. One can easily check that $(Y_k(p),Y_k(q))$ are jointly cyclostationary with a cyclic cross-correlation function expressed as

$$R^{\alpha}_{Y^{(p,q)}}(u) = E_s R^{\alpha}_{c^{(p,q)}}(u) H(p) H^*(q).$$

Finally, if we assume that M OFDM symbols are available at reception, the CCCF energy of $y_k(p)$ and $y_k(q)$ is evaluated thanks to the cost function defined as

$$J_{PIC} \triangleq \sum_{(p,q)\in\xi} \left(\sum_{\alpha\in\mathcal{A}_{(p,q)}} |\widehat{R}^{\alpha}_{\tilde{Y}^{(p,q)}}(d^{(p,q)})|^2 \right), \tag{8}$$

where

$$\widehat{R}^{\alpha}_{\tilde{Y}^{(p,q)}}(d^{(p,q)}) = \frac{1}{M-d^{(p,q)}} \sum_{k=0}^{M-d^{(p,q)}-1} \tilde{Y}_k(p) \tilde{Y}^*_{k+d^{(p,q)}}(q) e^{-i2\pi\alpha k} \tag{9}$$

and $\xi = \{(p,q) | \mathcal{A}_{(p,q)} \neq \emptyset \text{ and } d^{(p,q)} + K \leq M\}$. Note that in order to get the criterion J_{PIC} less sensitive to the received signal gain, each term $Y_k(n)$ in Eq. (9) is normalized so that

$$\tilde{Y}_k(n) = \frac{Y_k(n)}{\sqrt{\widehat{\mathrm{Var}}[Y(n)]}}, \tag{10}$$

where $\mathrm{Var}[\cdot]$ denotes the variance and

$$\widehat{\mathrm{Var}}[Y(n)] = \frac{1}{M} \sum_{k=0}^{M-1} |Y_k(n)|^2. \tag{11}$$

3.3.2. Decision statistics

Considering that a cognitive network ℓ to be detected embeds a known PIC signature $S^{(\ell)}$ and have a subcarrier spacing of $1/N^{(\ell)}$ and a cyclix prefix length of $D^{(\ell)}$, our detection problem can be formulated as a binary hypothesis test checking for the presence of cyclostationarity. Given $N^{(\ell)}$ and $D^{(\ell)}$,

$$\begin{cases} \mathcal{H}_0: & \forall (p,q,d^{(p,q)},K) \in S^{(\ell)},\ R^{\alpha}_{Y^{(p,q)}}(d^{(p,q)}) = 0, \\ \mathcal{H}_1: & \text{for some } (p,q,d^{(p,q)},K) \in S^{(\ell)},\ R^{\alpha}_{Y^{(p,q)}}(d^{(p,q)}) \neq 0. \end{cases} \tag{12}$$

To decide the most likely hypothesis, we propose a detection test constrained by the asymptotic false alarm rate (CFAR) quite similar to [36]. The decision is made by comparing J_{PIC} to a positive threshold such that

$$J_{PIC} \underset{\mathcal{H}_0}{\overset{\mathcal{H}_1}{\gtrless}} \Lambda,$$

with Λ defined as

$$\mathcal{F}_{J_{PIC}|\mathcal{H}_0}(\Lambda) = 1 - P_{fa}, \tag{13}$$

where $\mathcal{F}_{J_{PIC}|\mathcal{H}_0}$ is the cumulative distribution function (cdf) of J_{PIC} when $\mathcal{H}_0$ holds and P_{fa} is the tolerated false alarm probability.

The energy detector structure of the cost function J_{PIC} as well as the CFAR test is justified by the limited prior knowledge we have on the received signal. In fact, we cannot derive a detector structure or base our decision on the statistics of J_{PIC} under $\mathcal{H}_1$ as the latter depends on parameters such as the noise power or the propagation channel that are unknown at reception. Moreover, the detection is based on the knowledge of the pilot structure without the knowledge of pilot symbols so that the detection can be performed on every portion of the received signal. This leads to a short detection latency since there is no need for frame or superframe synchronization in contrast with coherent detection methods using known symbol sequences (see IEEE 802.22 [12]).

Since the multi-mode terminal cannot exhaustively know all the type of signals that will be fed into its detector (it only knows the features of the systems it is compatible with), in order to derive the asymptotic

Please cite this article as: F.-X. Socheleau, et al., Cognitive OFDM system detection using pilot tones second and third-order cyclostationarity, Signal Process. (2010), doi:10.1016/j.sigpro.2010.07.003

properties of J_{PIC}, the CFAR test is based on the following assumption:

Assumption 1. Under $\mathcal{H}_0$, $Y_k(n)$ are assumed to be i.i.d. zero-mean random variables.

Assumption 1 is not very restrictive since the noise and the vast majority of digital modulated signals that do not match the PIC signature to be detected can be modeled as i.i.d. zero-mean random variables. However, for the CFAR test to be efficient, Assumption 1 implies that the number of possible PIC signatures is large enough to design OFDM systems satisfying $S^{(\ell)} \bigcap S^{(m)} = \emptyset$, $\forall \ell \neq m$.

In order to find a relevant threshold Λ to perform the detection, we hereafter derive the asymptotic statistical behavior of J_{PIC} under $\mathcal{H}_0$.

Theorem 2. *Under hypothesis $\mathcal{H}_0$, the cumulative distribution function of J_{PIC} can be expressed as Laguerre series of the form*

$$\mathcal{F}_{J_{PIC}|\mathcal{H}_0}(x) = \frac{e^{-x/2\omega}}{(2\omega)^{\zeta+1}} \frac{x^{\zeta}}{\Gamma(\zeta+1)} \sum_{k\geq 0} \frac{k! m_k}{(\zeta+1)_k} L_k^{(\zeta)}\left(\frac{(\zeta+1)x}{2\omega v}\right),$$

$\forall v > 0$ *and* $\omega > 0$,

with $\zeta = \sum_{(p,q)\in\xi} \mathrm{card}(\mathcal{A}_{(p,q)})$ *and* $L_k^{(\zeta)}$ *the k-th generalized Laguerre polynomial verifying*

$$L_k^{(\zeta)}(x) \triangleq \sum_{m=0}^{k} \binom{k+\zeta}{k-m} \frac{(-x)^m}{m!}.$$

$\Gamma(x) \triangleq \int_0^{\infty} t^{x-1} e^{-t}\, dt$ *and* $(\cdot)_k$ *denotes the Pochhammer symbol defined as* $(x)_k \triangleq \Gamma(x+k)/\Gamma(x)$. *The coefficients* m_k *satisfy the following recurrent relation*:

$$m_k = \frac{1}{k} \sum_{j=0}^{k-1} m_j g_{k-j}, \quad k \geq 1$$

with

$$m_0 = 2(\zeta+1)^{\zeta+1} \frac{\omega^{\zeta+1}}{\zeta+1-v} \prod_{(p,q)\in\xi} \left(\omega v + \frac{\zeta+1-v}{2(M-d^{(p,q)})}\right)^{-\mathrm{card}(\mathcal{A}_{(p,q)})}$$

and

$$g_j = \left(\frac{-v}{\zeta+1-v}\right)^j + \sum_{(p,q)\in\xi} \mathrm{card}(\mathcal{A}_{(p,q)}) \left(\frac{v(2(M-d^{(p,q)})\omega - 1)}{2(M-d^{(p,q)})\omega v + \zeta + 1 - v}\right)^j,$$

$j \geq 1$.

Proof of Theorem 2 is given in Appendix B.

Note that the Laguerre expansion depends on v and ω that can be arbitrarily chosen, for more details refer to [37]. The choice of these parameters only have an impact on the convergence speed and uniformity. Moreover, for computer implementation, the Laguerre expansion has to be truncated. The number of terms to consider within the series can be estimated using the truncation error analytical expression given in [37]. For instance, only 15 terms are needed to get a proper estimate of the cdf under $\mathcal{H}_0$ in the situation illustrated in Fig. 4 by setting $M=50$, $v=3$ and $\omega \simeq 0.206$. Finally, as there are no known analytical solutions to invert the cdf of $J_{PIC}|\mathcal{H}_0$, the threshold Λ is approximated using classical iterative methods (Newton, etc.).

It is important to note in Theorem 2 that Λ only depends on the PIC signature design and on the observation window length. It is not impacted by environmental parameters such as signal power, propagation channel, etc. Therefore, Λ has just to be computed once "off-line" and then stored in a look-up table of the multi-mode terminal.

3.4. Discussion on the synchronization and channel impact on the PIC detector

3.4.1. Effect of synchronization impairments

As stated previously, it is unrealistic to consider the multi-mode terminal perfectly synchronized with the systems is trying to detect since it cannot know a priori ε, τ and θ (see Eq. (3)). It is straightforward to show that the phase shift θ has no effect on the cost function J_{PIC} since the detector is based on the CCCF energy estimation. However, timing missynchronization and/or frequency offset deteriorate the observations $Y_k(n)$ as inter-symbol (ISI) and inter-carrier (ICI) interferences occur [38–40], and therefore directly impact the cost function J_{PIC}. This is illustrated in Fig. 5 where the value of J_{PIC} is plotted for different frequency and timing offsets using a signal model similar to the one depicted in Section 5.2. The SNR is set to 0 dB, $M=24$ and the channel is frequency selective with a root mean square (RMS) delay spread equal to a quarter of the CP length. To guarantee the best detection performance, it is required to mitigate the time and frequency offset. Since the proposed detector does not rely on frame synchronization, the search interval for τ is limited to $[-0.5(N+D),\ 0.5(N+D))$. For ε, the search interval is system dependent. In an operational scenario similar to the context depicted by the 802.22 wireless group [13], the cognitive networks are frequency channelized which means that they can only transmit on a finite set of carrier frequencies known by the receiver. Therefore, when sensing a possible active channel, the cognitive terminal has only to mitigate the frequency offset due to the oscillator drift and to the Doppler effect. Depending on the oscillator precision, the frequency band and the terminal mobility, this offset is usually within the range of few times the subcarrier spacing.

Since existing blind OFDM synchronization methods [41–43] limit the frequency offset correction to plus or minus half the subcarrier spacing, they cannot be used in our context. In order to guarantee the best performance and to facilitate the communication link establishment that follows detection, we suggest to estimate (ε,τ) thanks to J_{PIC}. Fig. 5 shows that J_{PIC} is maximum for $\varepsilon = 0$ (no ICI) and $\tau = 0$ (no ISI) which leads to the following estimator:

$$[\widehat{\varepsilon},\widehat{\tau}] = \underset{(\varepsilon,t)}{\mathrm{argmax}} J_{PIC}^{(\varepsilon,t)}, \tag{14}$$

where $J_{PIC}^{(\varepsilon,t)}$ is defined as in Eq. (8) by replacing $Y_k(n)$ by

$$Y_k^{(\varepsilon,t)}(n) \triangleq \frac{1}{\sqrt{N}} \sum_{m=0}^{N-1} y[k(N+D)+D+m+t] e^{-2i\pi(nm/N-\varepsilon)}. \tag{15}$$

Detection and synchronization are thus jointly performed.

Please cite this article as: F.-X. Socheleau, et al., Cognitive OFDM system detection using pilot tones second and third-order cyclostationarity, Signal Process. (2010), doi:10.1016/j.sigpro.2010.07.003

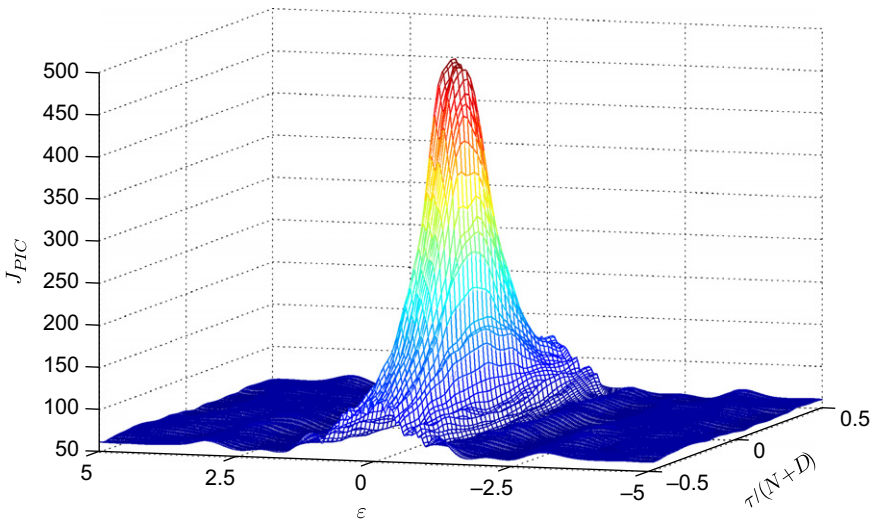

Fig. 5. Effect of synchronization impairments on the cost function J_{PIC} (SNR=0 dB, M=24, $\beta = 0.25D$).

As the channel is unknown at reception, the analytical expression of the derivative of $J_{PIC}^{(\varepsilon,t)}$ cannot be calculated. The optimization problem of Eq. (14) has therefore to be solved using an algorithm that only requires function evaluations and not derivatives. There are quite a few optimization methods in the literature that address this problem. For instance, there is the downhill simplex method due to Nelder and Mead [44] but it is not very efficient in terms of the number of function evaluations that it requires. Powell's method [45] or the Davidon–Fletcher–Powell method with finite differences [46, Chapter 10.9] are almost surely faster. For the simulations in Section 5, we use Powell's algorithm which is known as one of the conjugate direction algorithms. Conjugate directions have the special property that minimization along one direction is not "spoilt" by subsequent minimization along another, so that interminable cycling through the set of directions can be avoided (see [46, Chapter 10.7] for more details). Experiments show that this method only requires 50–100 iterations to converge over a search window of $[-0.5(N+D), 0.5(N+D))$ for t and $[-10, 10]$ for ε.

The solution of Eq. (14) obviously results in a computational burden increase. However, in a cognitive radio context, this additional complexity *is not prohibitive* compared to classical preamble matched filter detection. If we still consider the IEEE 802.22 cognitive system as a reference, for each sensed channel, the superframe preamble matched filter detection would require terminals to perform a sliding cross-correlation over 80 ms on average if the channel is active and over 160 ms if the channel is inactive. This has to be compared with the PIC detection scheme that only requires a signal duration of a few ms (see Section 5) whatever the state of the channel may be (active or inactive). Consequently, even if the computational cost per signal sample of the PIC method is higher than the matched filter detection, since the total number of samples to be processed by the PIC method is much smaller than the other method, the overall PIC complexity is still acceptable.

For instance, in the case of preamble detection based on a matched filter, the complexity is $N \times (T\text{-}1)$ multiplication-accumulations (MAC) for each sensed channel, where T is the number of samples in the observation window. For a typical IEEE 802.22 scenario with a 6 MHz active channel, N=2048 and T=0.08 × 6.10^6 (on average) which induces a complexity of approximately 9.8×10^8 MAC. As for the proposed detector, for each sensed channel and at each iteration of the Powell algorithm, it performs M FFT and then correlates the card(ξ) pilot pairs that define the signature. The overall complexity is therefore $(M \times N\log_2 N + \text{card}(\xi) \times M) \times Q$, where Q is the total number of iterations needed for the Powell algorithm to converge. As shown in Section 5, the detector offers good performance for M=24, card(ξ) = 30 and Q=100. This results in a complexity of approximately 5.4×10^7 MAC.

Moreover, we recall that pilot tone-based detection methods have the major advantage of drastically reducing the detection latency relatively to matched filter detection. In addition, in the context described in this paper, requiring synchronization for detection is not unreasonable since at the end the multi-mode terminal will have to do it anyway to measure some metrics useful to decide whether to trigger a handoff or not [47, Chapter 20].

3.4.2. *Effect of frequency-selective channels*

The frequency selectivity of the propagation channel impacts the subcarrier-to-noise-ratio of the pilot tones as they are weighted by $H(n)$. However, similarly to the term $e^{i\varphi}$ in Theorem 1 or the initial phase shift θ, as long as the channel is time-invariant, the phase difference between $H(p)$ and $H(q)$ has strictly no effect on the performance since the detection is based on the CCCF energy. We recall that the impact of channel fluctuations is discussed in Section 5.

Please cite this article as: F.-X. Socheleau, et al., Cognitive OFDM system detection using pilot tones second and third-order cyclostationarity, Signal Process. (2010), doi:10.1016/j.sigpro.2010.07.003

4. *m*-Sequence signatures

PIC signatures present the major advantage of being easy to generate and to adapt to any specific pilot tones time–frequency distribution. However, such a signature scheme might not be compatible with cognitive systems that would use pilot tones for protocol signaling where correlation between pilot symbols cannot be guaranteed. Indeed, in some cases pilot subcarriers can carry system control information. For instance, solutions have been suggested to transmit coded vector mask on pilot subcarriers for PAPR minimization. In this case, pilot tones embed a pseudo-random sequence that is either used to inform the receiver of the mapping scheme selected[3] at the transmitter side [27], or chosen among a set of predefined sequences as the one that provides the lowest PAPR when combined with the data [28]. In the first case, pilot tones carry information whereas in the second they directly reduce the overall PAPR.

In both cases, the main requirement on these sequences is their (quasi-) orthogonality to ease the decoding at reception. The receiver only knows the set of predefined sequences but not the actual transmitted sequence. Decoding is thus performed by exhaustively testing all possible sequences for each OFDM symbol.

In this context, following the same progression as the previous section, we here develop a solution relying on the use of *m*-sequence (MS) modulated pilot tones to embed signatures in OFDM signals. MS are widely spread in wireless systems for operation such as scrambling, spectrum spreading or channel estimation [32,34]. As detailed hereafter, MS are of great interest since they show specific higher-order statistics relevant for system detection and meet the (quasi-)orthogonality or low cross-correlation requirements.[4]

This section is organized as follows: the basic properties of MS are first recall in Section 3.1. We then define what we call a MS signature in Section 4.2. A detector tailored to the proposed signature scheme is detailed in Section 4.3. For the same reasons as for the PIC detector, perfect synchronization is first implicitly admitted to derive the cost function. Finally, some methods to mitigate the propagation channel and synchronization impairments are discussed in Section 4.4.

4.1. Background on m-sequence

A maximum length sequence, commonly called *m*-sequence, is a type of pseudo-random binary sequence generated using maximal linear feedback shift registers and modulo 2 addition. A necessary and sufficient condition that a sequence be of maximal length (i.e. sequence of length 2^p-1 for length-p registers) is that its corresponding generator polynomial, denoted by P_{MS}, be primitive. Such sequences satisfy the following properties [48].

Property 1. *Let w_k be a binary MS of length 2^p-1 and $\breve{w}_k=1-2w_k$ its BPSK associated sequence, the autocorrelation function of $\breve{w}_k$ is given by*

$$\Psi(k)=\frac{1}{2^p-1}\sum_{i=0}^{2^p-2}\breve{w}_i\breve{w}_{k+i}=\begin{cases}1 & \text{if } k=0,\\ 1/(1-2^p) & \text{otherwise.}\end{cases}$$

Property 2. *Any binary MS w_k generated by length p registers of polynomial $P_{MS}=\sum_{i=0}^{p}\alpha_i X^i$ verifies over GF(2)*

$$w_k=\sum_{i=1}^{p}\alpha_i w_{k-i} \;\Leftrightarrow\; \sum_{i=0}^{p}\alpha_i w_{k-i}=0$$

that can also be written as

$$\prod_{i\in\mathcal{C}}\breve{w}_{k-i}=1$$

where $\mathcal{C}=\{i\in\{0,\ldots,p\}|\alpha_i=1\}$.

Property 3. *If $w(k)$ is a MS then $w(k)\oplus w(k+i)$ is also a MS $\forall i$, with $\oplus$ the addition in GF(2). Considering Property 1, this leads to*

$$\lim_{M\to+\infty}\frac{1}{M}\sum_{k=0}^{M-1}\left(\prod_{i\in\mathcal{B}}\breve{w}_{k-i}\right)=\frac{1}{1-2^p},\quad \forall\mathcal{B}\neq\mathcal{C}, \tag{16}$$

where $\mathcal{B}$ is any subset of $\{0,\ldots,2^p-2\}$.

Property 4. *All non-zero codewords have an identical Hamming distance equal to 2^{p-1}.*

These properties show that MS are good candidates for protocol signaling as they have low cross-correlation values. Moreover, MS show a convolution property (Property 2) that can be exploited for system identification.

4.2. m-Sequence (MS) pattern generation

In order to facilitate the identification of OFDM systems, we suggest to generalize the use of MS when protocol signaling through pilot subcarriers is needed. In this case, for each k, $b_k(n)$ in Eq. (2) is a BPSK pilot symbols sequence associated with one MS obtained by the generator polynomial P_{MS}. To facilitate the identification and avoid too complex detection statistics, we limit P_{MS} to trinomials of the form $1+X^l+X^p$ ($p>l$). This limitation has no impact on the signaling properties since the cross-correlation and the Hamming distance only depend on the polynomial degree and not on the cardinal of $\mathcal{C}$. System signature is thus entirely characterized by $\cup_{k\in\mathbb{Z}}\mathcal{I}(k)$ and P_{MS}.

4.3. m-Sequence pattern detection

4.3.1. Detection cost function

Our objective is now to propose a cost function to detect MS signatures. Contrary to protocol signaling

[3] In the selected mapping (SLM) approach, the input data frame is multiplied by a finite number of random sequences and whichever resultant sequence has the lowest PAPR is then selected for transmission. To enable the receiver to recover the data, a pointer to the multiplying sequence is transmitted as side information carried by the pilot tones.

[4] Note that in the example [27] given previously, the side information is coded using *m*-sequences and that *m*-sequences can also be shown to be good candidates for the PAPR reduction method proposed in [28].

Please cite this article as: F.-X. Socheleau, et al., Cognitive OFDM system detection using pilot tones second and third-order cyclostationarity, Signal Process. (2010), doi:10.1016/j.sigpro.2010.07.003

decoding that usually consists of testing, for each OFDM symbol, all possible codewords to decide which one is the most likely, we here propose to limit the complexity by verifying whether the codewords have been generated by the right P_{MS}. If we consider systems with equispaced pilot subcarriers, from the properties depicted in the previous subsection it comes that the pilot symbols $b_k(n)$ verify

$$b_k(n)b_k(n-l\Delta)b_k(n-p\Delta)=1, \quad \forall n \in \{\mathcal{I}(k)|n \geq p\Delta\}, \tag{17}$$

where Δ denotes the number of subcarriers between pilot tones. Thus, for equipowered subcarriers, by analogy with the PIC criterion, we define

$$C_k^\alpha(l,p,\Delta) \triangleq \sum_{n=p\Delta}^{N-1} \mathbb{E}[c_k(n)c_k^*(n-l\Delta)c_k(n-p\Delta)]e^{-i2\pi\alpha n}.$$

From Eq. (17) and assuming i.i.d. data symbols

$$\mathbb{E}[c_k(n)c_k^*(n-l\Delta)c_k(n-p\Delta)] = \sum_{m=p}^{\lfloor (N-1-n_0(k))/\Delta \rfloor} \delta[n-m\Delta-n_0(k)],$$

where $\delta[\cdot]$ is the Kronecker delta and $n_0(k)$ denotes the subcarrier index of the first pilot on symbol k. It follows that

$$\begin{aligned} C_k^\alpha(l,p,\Delta) &= \sum_{n=p}^{\lfloor (N-1-n_0(k))/\Delta \rfloor} e^{-i2\pi\alpha(n\Delta+n_0(k))} \\ &= \frac{\sin\left(\pi\alpha\Delta\left(\left\lfloor\frac{N-1-n_0(k)}{\Delta}\right\rfloor-p\right)\right)}{\sin(\pi\alpha\Delta)} e^{-i\pi\alpha\Delta(\lfloor (N-1-n_0(k))/\Delta \rfloor-p)}. \end{aligned}$$

Hence, $\{c_k(n)\}_n$ is third-order cyclostationary since $C_k^\alpha(l,p,\Delta)$ shows peak of energy for $\alpha \in \mathcal{A}$, with $\mathcal{A}=\{(m-\lfloor \Delta/2 \rfloor)/\Delta,\ m \in \{0,1,\ldots,\Delta-1\}\}$. The system specific signature is then defined as

$$S \triangleq \{(l,p,\Delta)|\mathcal{A} \neq \emptyset\} \quad \text{given } N \text{ and } D. \tag{18}$$

Consequently, we build a cost function J_{MS} based on third-order statistics defined as

$$J_{MS} \triangleq \sum_{k=0}^{M-1} \left(\sum_{\alpha \in \mathcal{A}} |\widehat{C}_k^\alpha(l,p,\Delta)|^2 \right), \tag{19}$$

where

$$\widehat{C}_k^\alpha(l,p,\Delta) \triangleq \frac{1}{N-p\Delta} \sum_{n=p\Delta}^{N-1} \tilde{Y}_k(n)\tilde{Y}_k^*(n-l\Delta)\tilde{Y}_k(n-p\Delta)e^{-i2\pi\alpha n}.$$

Note that only considering equispaced pilot subcarriers does not limit much our criterion as most systems verify this property thanks to the result on the optimal pilots location presented in [29]. However, to enlarge the scope of the proposed signature scheme, the cost function of Eq. (19) can easily be adapted to non-equispaced pilot subcarriers by considering

$$\check{C}_k^\alpha(l,p) \triangleq \frac{1}{\mathrm{card}(\mathcal{I}(k))} \sum_{n_i \in \mathcal{I}(k)} \tilde{Y}_k(n_i)\tilde{Y}_k^*(n_{i-l})\tilde{Y}_k(n_{i-p})$$

instead of $\widehat{C}_k^\alpha(l,p,\Delta)$ and with $\mathcal{A}=\{0\}$. Nevertheless, for the sake of simplicity, we present derivation and simulation results associated with Eq. (19).

4.3.2. Decision statistics

We here conduct a hypothesis test similar to Section 3.3.2. Considering that a cognitive network ℓ to be detected embeds a known MS signature $S^{(\ell)}$ and given $N^{(\ell)}$ and $D^{(\ell)}$, $\mathcal{H}_0$ and $\mathcal{H}_1$ are defined as

$$\begin{cases} \mathcal{H}_0: & \forall k \text{ and } (l,p,\Delta) \in S^{(\ell)},\ C_k^\alpha(l,p,\Delta)=0, \\ \mathcal{H}_1: & \text{for some } k \text{ and } (l,p,\Delta) \in S^{(\ell)},\ C_k^\alpha(l,p,\Delta) \neq 0. \end{cases} \tag{20}$$

Using the same CFAR test as in Section 3.3.2, we now have derive the cdf of $J_{MS}|\mathcal{H}_0$ to get the decision threshold. Note that for the same reason as in Section 3.3.2, $\mathcal{H}_0$ embodies the vast majority of digital modulated signals. However, in the specific case of $\mathcal{H}_0$ where an OFDM system has the same parameters N,D,Δ as the system to detect but with a MS structure of a different polynomial P'_{MS} of degree p', Property 3 indicates that using a CFAR detector can be a concern. In this case the asymptotic distribution of $J_{MS}|\mathcal{H}_0$ is dependent on p' which is not necessarily known by the multi-mode terminal. The terminal only knows the parameters of the systems it is compatible with. For instance, for $\mathrm{card}(\mathcal{I}(k)) \to +\infty$ and in the purely theoretical scenario where the receiver is perfectly synchronized

$$C_k^\alpha(l',p',\Delta) = \frac{C_k^\alpha(l,p,\Delta)}{1-2^{p'}} \neq 0. \tag{21}$$

Thus, without the knowledge of p' we cannot choose a threshold that guarantees a given P_{fa}. The only way to overcome this problem is to choose an empirical default value of the degree p'. For the sake of simplicity, we consider that $p'=+\infty$. Impacts of this assumption on performance are discussed in Section 5.

Following exactly the same reasoning as in Appendix B, under $\mathcal{H}_0$ it comes that the coefficients $\widehat{C}_k^\alpha(l,p,\Delta)$ are zero-mean asymptotic uncorrelated Gaussian variables of variance $1/(N-p\Delta)$. Then, the characteristic function of $J_{MS}|\mathcal{H}_0$ is expressed as

$$\psi_{J_{MS}|\mathcal{H}_0}(t) = \left(1-\frac{it}{N-p\Delta}\right)^{-\Delta M}$$

which leads to the following theorem.

Theorem 3. *Under hypothesis $\mathcal{H}_0$, the asymptotic cumulative distribution function of $J_{MS}|\mathcal{H}_0$ is expressed as*

$$\mathcal{F}_{J_{MS}|\mathcal{H}_0}(x) = \frac{\gamma(\Delta M,(N-p\Delta)x)}{(\Delta M-1)!},$$

where $\gamma(a,x)$ is the incomplete gamma function defined as $\gamma(a,x) \triangleq \int_0^x t^{a-1}e^{-t}\,dt$.

The decision threshold can now be computed thanks to the previous theorem.

4.4. Discussion on the synchronization and channel impacts on the MS detector

4.4.1. Effect of synchronization impairments

Like the PIC criterion, the cost function J_{MS} is affected by ISI and ICI interferences resulting from missynchronization. As J_{MS} is built on third-order statistics, the attenuation factor imputable to missynchronization is stronger than for J_{PIC}. Moreover, it can be shown that

Please cite this article as: F.-X. Socheleau, et al., Cognitive OFDM system detection using pilot tones second and third-order cyclostationarity, Signal Process. (2010), doi:10.1016/j.sigpro.2010.07.003

timing synchronization errors shift the cyclic frequencies which results in additional attenuation of the power of $\widehat{C}_k^{\alpha}(l,p,\Delta)$ for $\alpha \in \mathcal{A}$. Therefore, it is strongly recommended to estimate ε and τ.

Similarly to the PIC criterion, J_{MS} is maximum in the case of perfect synchronization which leads to the following estimator:

$$[\widehat{\varepsilon},\widehat{\tau}] = \underset{(\varepsilon,t)}{\operatorname{argmax}} J_{MS}^{(\varepsilon,t)}, \tag{22}$$

where $J_{MS}^{(\varepsilon,t)}$ is defined as in Eq. (19) by replacing $Y_k(n)$ by $Y_k^{(\varepsilon,t)}(n)$ defined in Eq. (15). Note that contrary to the PIC criterion, J_{MS} only depends on the fractional part of ε (see Eq. (19), so that $J_{MS}^{(\varepsilon,t)} = J_{MS}^{(\varepsilon+k,t)}, k \in \mathbb{Z}$. This means that existing blind OFDM synchronization methods [41–43] that usually consider a frequency offset within $[-0.5, 0.5)$ could also be used prior to MS detection (refer to Section 5 for more details).

4.4.2. Effect of frequency-selective channels

In contrast with the PIC criterion, the propagation channel is an important element to consider here as it can have a strong impact on the MS cost function. For instance, in the case of a frequency selective channel we can have situations where the different $H(n)$ can be considered as random variables verifying

$$\mathbb{E}[H(n)H^*(n-l\Delta)H(n-p\Delta)] = 0 \Rightarrow \mathbb{E}[\widehat{C}_k^{\alpha}(l,p,\Delta)] = 0.$$

This makes the detection impossible. One way to overcome this problem is to estimate and compensate the phase shift imputable to the channel. In this case, it can be shown that the cost function only gets deteriorated by the SNR loss due to propagation. The phase shift can be estimated using Eq. (17). If we write $H(n)$ as $H(n) = |H(n)|e^{i\theta(n)}$ and assume perfect synchronization and a noiseless channel, Eq. (17) yields the following relation for $\Theta(n,l,p,\Delta) \triangleq \theta(n) - \theta(n-l\Delta) + \theta(n-p\Delta)$,

$$\Theta(n,l,p,\Delta) = \arg[\tilde{Y}_k(n)\tilde{Y}_k^*(n-l\Delta)\tilde{Y}_k(n-p\Delta)], \quad \forall n \in \mathcal{I}(k). \tag{23}$$

Notice that the equation system (23) is under-determined since there are $\operatorname{card}(\mathcal{I}(k))$ unknown for $\operatorname{card}(\mathcal{I}(k)) - p$ equations. This is not a concern as any solution will have exactly the same impact on J_{MS}. Therefore, it only suffices to choose one possible solution to compensate the performance loss imputable to the channel phase. In practice, Eq. (23) cannot be applied as such since the receiver is not synchronized. This limitation can be addressed in two steps. First, we slightly relaxed the perfect synchronization assumption by considering that the receiver is still symbol and frequency synchronized but not frame synchronized anymore. Thus, the receiver cannot know $\mathcal{I}(k)$ for each symbol k. One way to overcome this lack of knowledge is to exploit the fact that $\mathcal{I}(k) = \mathcal{I}(k+K)$ and that $\theta(n)$ is invariant in k (under the time invariant channel assumption). In this case, $\Theta_k(n,l,p,\Delta)$ can be estimated as

$$\widehat{\Theta}_k(n,l,p,\Delta) = \arg\left[\frac{1}{\lfloor M/K \rfloor - k} \sum_{\substack{m=0 \\ \lfloor k \rfloor_K + Km \neq k}}^{\lfloor M/K \rfloor - 1 - k} \tilde{Y}_{\lfloor k \rfloor_K + Km}(n)\tilde{Y}^*_{\lfloor k \rfloor_K + Km}(n-l\Delta), \times \tilde{Y}_{\lfloor k \rfloor_K + Km}(n-p\Delta)\right], \tag{24}$$

where $[\,\cdot\,]_K$ denotes the modulo K operation. Finally, to fully relax the perfect synchronization assumption, $\widehat{\Theta}_k(n,l,p,\Delta)$ is jointly computed with the maximization of $J_{MS}^{(\varepsilon,t)}$ in Eq. (22). That is to say that for every tested pair (ε,t), $\Theta(n,l,p,\Delta)$ is estimated thanks to Eq. (24).

5. Simulations

5.1. Simulation context

In the following, all the results are averaged over 1000 Monte-Carlo runs. We consider 512-subcarrier OFDM systems inspired from the Mobile WiMAX [26] with D=64, 60 pilot, 360 data, 91 guard and 1 DC subcarrier. The subcarriers are equipowered. The Signal-to-Noise Ratio (SNR) is defined as $\mathrm{SNR(dB)} = 10\log_{10}(E_s/\sigma^2)$. The simulated propagation channel is a discrete-time frequency selective channel $\{h_k(l)\}_{l=0,\ldots,L}$ with L=D and an exponential decay profile for its non-null component (i.e. $\mathbb{E}[|h_k(l)|^2] = Ge^{-l/\beta}$ for l=0,…, L and G is chosen such that $\sum_{l=0}^{L} \mathbb{E}[|h_k(l)|^2] = 1$). Notice that β approximately corresponds to the root mean square (RMS) delay spread. We recall that $\{h(l)\}_{l=0,\ldots,L-1}$, ε, θ, τ, σ^2, $a_k(n)$ and $b_k(n)$ are unknown at reception. The probability of detection is defined as

$$P_{det} = P[J_{PIC \text{ or } MS} > \Lambda | \mathcal{H}_1].$$

For the simulations, uniformly distributed random ε and τ are generated with $-10 \le \varepsilon \le 10$ which corresponds to a carrier frequency offset of ± 10 times the subcarrier spacing and with $-0.5(N+D) \le \tau < 0.5(N+D)$. The optimization problems of Eqs. (14) and (22) are solved using the conjugate direction method of Powell that searches the maximum of an objective function without calculating its derivative [45]. In order to keep the false alarm rate to the expected value, maximizing the cost function implies to change the detection threshold. In fact, if Powell's algorithm converges after Q iterations and we assume that under $\mathcal{H}_0$ the cost function values are independent from an iteration to another, then the detection threshold has to verify

$$(\mathcal{F}_{J_{PIC \text{ or } MS}|\mathcal{H}_0}(\Lambda))^Q = 1 - P_{fa}.$$

The limit the computational complexity, Q is upper-bounded by 100 in all the simulations presented hereafter.

5.2. PIC signature detection performance

To evaluate the PIC signature detection performance, we induce joint cyclostationarity on 30 pilot pairs with $d^{(p,q)}$=2 and q=p+210 for any admissible (p,q).

Please cite this article as: F.-X. Socheleau, et al., Cognitive OFDM system detection using pilot tones second and third-order cyclostationarity, Signal Process. (2010), doi:10.1016/j.sigpro.2010.07.003

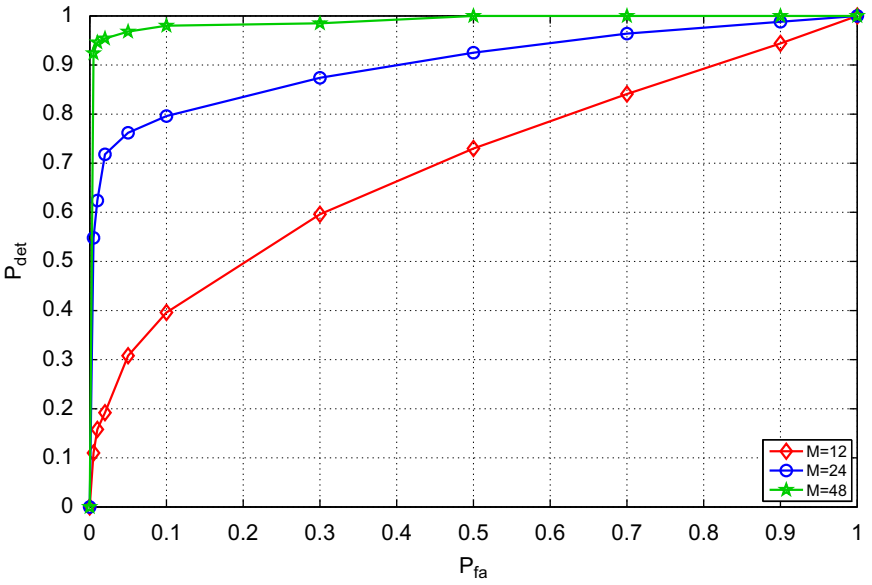

Fig. 6. PIC criterion—receiver operating characteristic with an increasing length of the observation window ($\beta = 0.25D$, SNR= -5 dB).

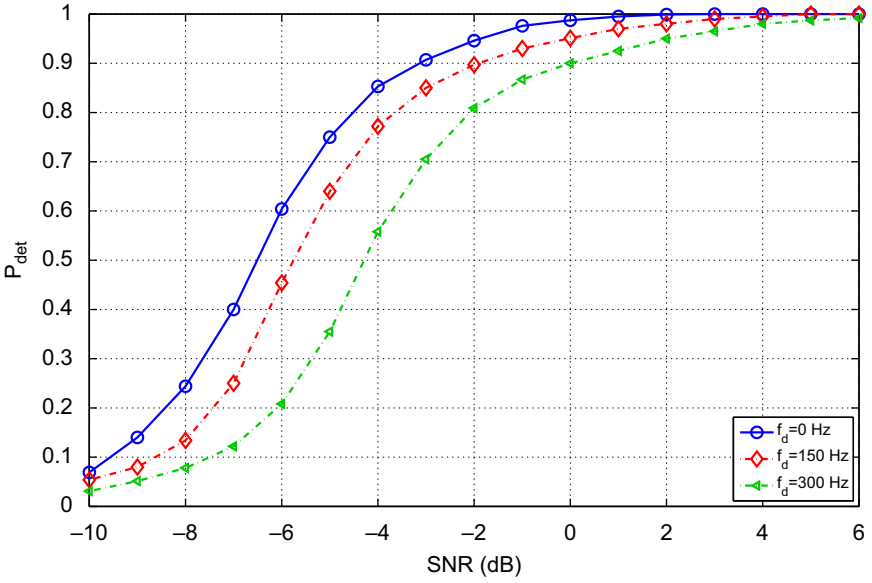

Fig. 7. PIC criterion—effect of Doppler spread on the correct detection probability (M=24, $\beta = 0.25D$, P_{fa}=0.02).

In Fig. 6, we plot the receiver operating characteristics (ROC) for various observation window lengths and for a SNR= -5 dB. The tested observation window lengths have been chosen to avoid long sensing period in scenarios where cognitive networks can operate in several frequency channels. For instance, 12 WiMAX OFDM symbols only correspond to a duration of 1.23 ms. In Fig. 6, we observe that the detection rate is significantly improved as the number of available symbols increases. However, it can be seen that the relative performance improvement diminishes as the observation window gets larger.

Fig. 7 highlights the impact of the frequency-selective channel when it becomes time-variant. Time variation is simulated using Jakes model. Various values of maximum Doppler frequencies f_d have been inspected for a false alarm rate set to 2%. It can be seen that our algorithm is quite robust to Doppler spread. For f_d=300 Hz (at 3 GHz, this corresponds to a relative velocity of 108 kph), there is a loss up to 4 dB but the detection performance is still excellent in the standard SNR operating range[5] for a mobile environment.

[5] SNR range where OFDM based systems experience bit-error rates low enough to operate.

Please cite this article as: F.-X. Socheleau, et al., Cognitive OFDM system detection using pilot tones second and third-order cyclostationarity, Signal Process. (2010), doi:10.1016/j.sigpro.2010.07.003

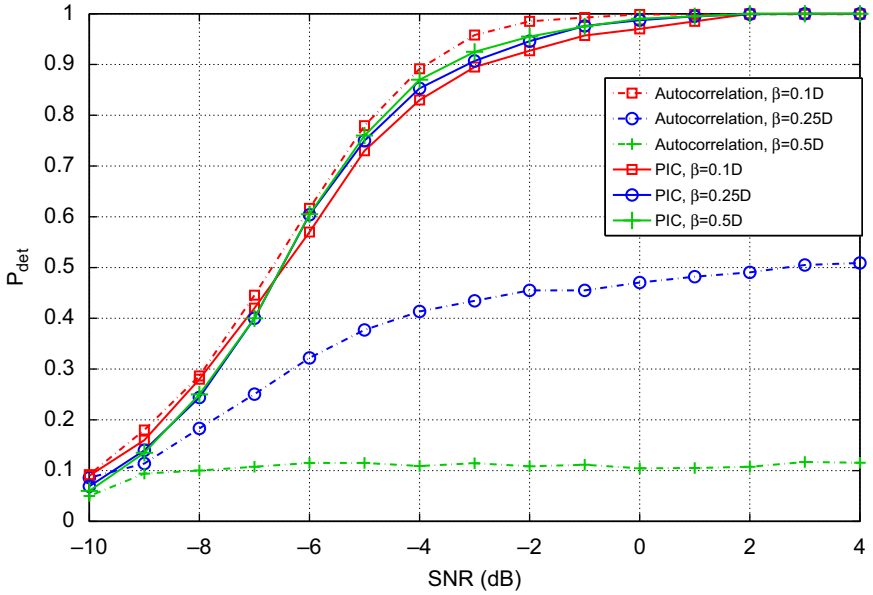

Fig. 8. PIC criterion—comparison between the PIC and the autocorrelation methods (M=24, P_{fa}=0.02).

As stated in the Introduction, most existing OFDM detection methods rely on the correlation induced by the cyclic prefix (see [17–19] for instance). In Fig. 8, we compare the correct detection probability versus SNR between the proposed PIC criterion and the standard autocorrelation based method for various channel RMS delay spread. To compare both methods, we consider that the correlation-based detection is correct when

$$N-\delta/2 \le \underset{\nu\in[\nu_{min},\nu_{max}]}{\operatorname{argmax}} \left| \sum_{m=0}^{M'-\nu-1} y(m)y^*(m+\nu) \right| \le N+\delta/2,$$

where $M'=M(N+D)$, ν_{min}=32 and ν_{max}=2048 which corresponds to searching systems from 32 to 2048 subcarriers, and where δ is the tolerated error on the estimation. We choose δ to be conditioned by the P_{fa} under the white Gaussian noise hypothesis such that $\delta=(\nu_{max}-\nu_{min})P_{fa}$. As expected, the correlation algorithm completely falls down as soon as the channel becomes somewhat selective whereas the PIC method is clearly robust to frequency selectivity. Moreover, we recall that the PIC criterion can discriminate systems with the same OFDM modulation parameters whereas the correlation algorithm cannot.

5.3. MS signature detection performance

To validate the m-sequence signature scheme, equispaced pilot tones with $\Delta=7$ are simulated. We apply MS of polynomial $1+X^2+X^5$ that generates codewords of length 31 satisfying $2^p-1 \le \mathrm{card}(\mathcal{I}(k))$ (p=5, $\mathrm{card}(\mathcal{I}(k))=60$).

To set a relevant detection threshold, we first evaluate the specific case of $\mathcal{H}_0$ where an OFDM system has the same parameters N,D,Δ as the system to detect but with a MS structure of a different polynomial P'_{MS} of degree p' (see Section 4.3.2). Simulation results (not shown here) indicate that in a realistic context, like the one depicted in this section, considering $p'=+\infty$ has strictly no impact on the performance. In fact, whatever the SNR and the tested polynomial (different from $1+X^2+X^5$) may be, the false alarm rate obtained by the Monte-Carlo runs is always around the value set for P_{fa} and not higher. This finds an explanation in the synchronization and channel phase estimation procedure. Without the right polynomial knowledge, the receiver is unable to get synchronized and to compensate the channel phase shift using Eqs. (22) and (24). Therefore, the detection threshold can be set without any knowledge of p' as it will not impact the performance.

Fig. 9 presents the receiver operating characteristics for various observation window lengths and for a SNR=4 dB. Similarly to the PIC criterion, MS performance is improved in parallel with the increase of the number of available symbols.

Fig. 10 shows the channel Doppler spread effect on the MS criterion. First, it can be seen that the MS criterion is less effective than the PIC criterion. Using 3rd order statistics makes the detection algorithm more sensitive to noise than a 2nd order based criterion. Moreover, the phase estimator of Eq. (23) is very sensitive to SNR when only few symbols are available to average the estimate. However, the MS method still performs well for low Doppler in the SNR range of interest. We recall that in contrast with licensed user detection, cognitive system detection is mostly required to have good performance in SNR ranges where systems experience bit error rates low enough to operate. Fig. 10 also indicates that the MS criterion is quite robust to Doppler spread below 150 Hz and that performance degrades up to 3 dB for a Doppler of 300 Hz. The performance degradation is once again amplified by the channel phase estimator based on the time-invariant channel assumption.

As discussed in Section 4.4, the MS criterion is not affected by the integer part of the frequency offset ε so

Please cite this article as: F.-X. Socheleau, et al., Cognitive OFDM system detection using pilot tones second and third-order cyclostationarity, Signal Process. (2010), doi:10.1016/j.sigpro.2010.07.003

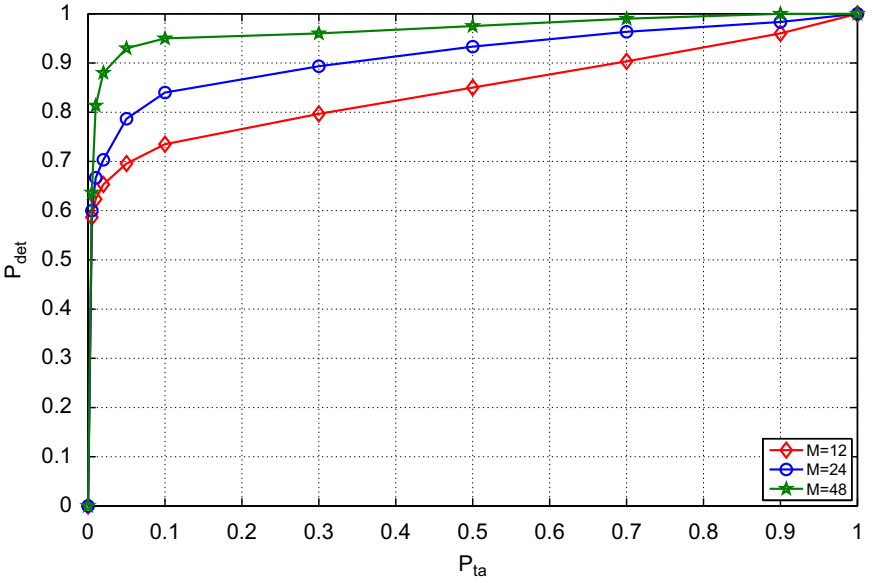

Fig. 9. MS criterion—receiver operating characteristic with an increasing length of the observation window ($\beta = 0.25D$, SNR=4 dB).

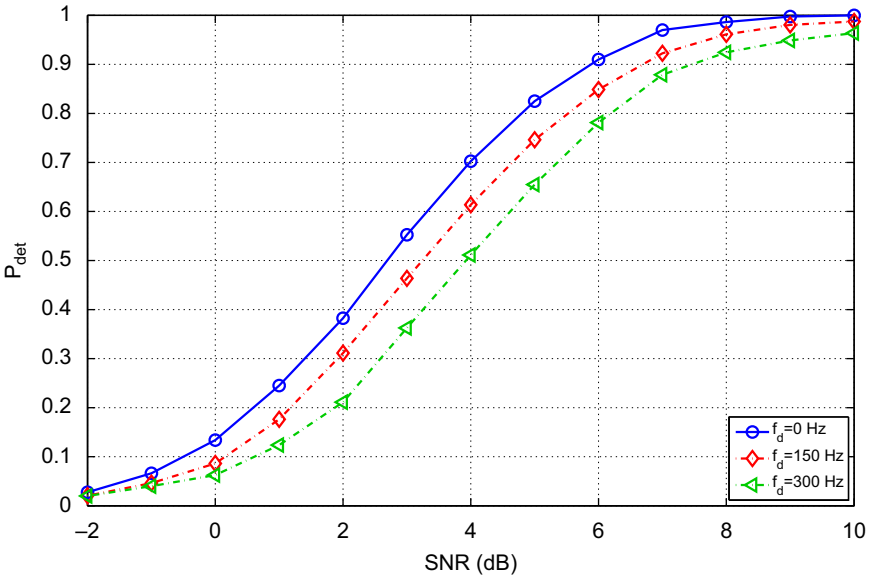

Fig. 10. MS criterion—effect of Doppler spread on the correct detection probability (M=24, $\beta = 0.25D$, f_d=0 Hz, P_{fa}=0.02).

that existing blind OFDM synchronization algorithms can be applied prior to detection. By comparing the algorithm suggested in Eq. (22) with the maximum likelihood estimator derived in [41], Fig. 11 shows the impact that the synchronization method can have on the detection performance. It can be seen that using Eq. (22) leads up to a 4 dB performance gain compared to maximum likelihood synchronization.

6. Conclusion

In this paper, we have introduced two new signature schemes to address the OFDM system detection challenge inherent to the vertical handoff process in a cognitive radio context. Both methods are based on patterns embedded onto pilot tones which has the main advantage of creating signatures easy to intercept, not adding any system overhead and making possible the discrimination of systems with similar modulation parameters. The signature schemes presented in this contribution consider existing pilot constraints in order to be compatible with most standard specifications.

The first scheme, relying on 2nd order joint cyclostationarity, is applicable to any system that has no specific requirements on the pilot symbol sequences. Simulations have demonstrated the detection efficiency of this kind of

Please cite this article as: F.-X. Socheleau, et al., Cognitive OFDM system detection using pilot tones second and third-order cyclostationarity, Signal Process. (2010), doi:10.1016/j.sigpro.2010.07.003

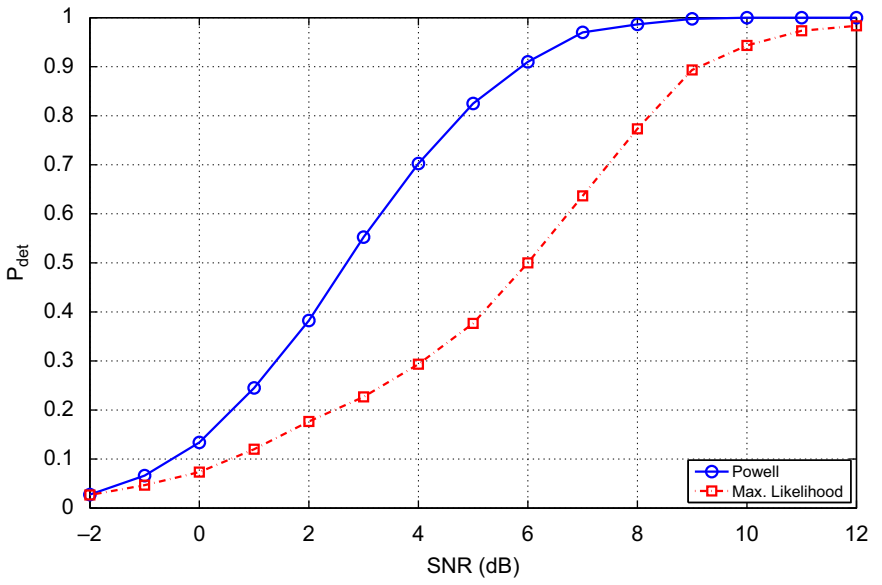

Fig. 11. MS criterion—impact of the synchronization method on the detection performance (M=24, $\beta = 0.25D$, P_{fa}=0.02).

pattern and have particularly shown its robustness to harsh propagation environment.

The second signature scheme, based on m-sequences, deals with the constraint of protocol signaling and also offers good performance however limited by the necessity to blindly mitigate the phase shift induced by the propagation channel. Robustness improvement may be a topic to consider in forthcoming work. More specifically, can we find other codes that are compliant with protocol signaling and system signature requirements while offering better detection performance than m-sequences?

Appendix A. Proof of Theorem 1

The CCCF of $c_k(p)$ and $c_k(q)$ is defined as

$$R^{\alpha}_{c^{(p,q)}}(u) \triangleq \lim_{M\to+\infty} \frac{1}{2M+1} \sum_{k=-M}^{M} \mathbb{E}[c_k(p)c^*_{k+u}(q)]e^{-i2\pi\alpha k}.$$

The data symbols $a_k(n)$ being i.i.d. and $b_k(p) = b_{k+d^{(p,q)}}(q)e^{i\varphi}$, it follows that

$$\mathbb{E}[c_k(p)c^*_{k+d^{(p,q)}}(q)] = \sigma_b^2 e^{-i\varphi} \sum_{\ell\in\mathbb{Z}} \delta[k-\ell K-k_0],$$

where $\delta[\cdot]$ is the Kronecker delta, σ_b^2 is the variance of symbols $b_k(n)$ and k_0 is the index of the first OFDM symbol embedding pilot tones. Hence,

$$R^{\alpha}_{c^{(p,q)}}(d^{(p,q)}) = \frac{\sigma_b^2 e^{-i(2\pi\alpha k_0+\varphi)}}{K} \sum_{m\in\mathbb{Z}} \delta\left[\alpha - \frac{m}{K}\right].$$

Therefore, for $\alpha \in [-1/2; 1/2[$, $R^{\alpha}_{c^{(p,q)}}(d^{(p,q)}) \neq 0$ iff $\alpha \in \{(m-\lfloor K/2\rfloor)/K, m \in \{0,1,\ldots,K-1\}\}$.

Appendix B. Proof of Theorem 2

We first derive the expectation and variance of the CCCF $\widehat{R}^{\alpha}_{\tilde{Y}^{(p,q)}}(d^{(p,q)})$ defined in Eq. (9).

The expectation of $\widehat{R}^{\alpha}_{\tilde{Y}^{(p,q)}}(d^{(p,q)})$ is given by

$$\mathbb{E}[\widehat{R}^{\alpha}_{\tilde{Y}^{(p,q)}}(d^{(p,q)})] = \frac{1}{M-d^{(p,q)}} \sum_{k=0}^{M-d^{(p,q)}-1} \mathbb{E}[\tilde{Y}_k(p)\tilde{Y}^*_{k+d^{(p,q)}}(q)]e^{-i2\pi\alpha k}$$

$$= R^{\alpha}_{\tilde{Y}^{(p,q)}}(d^{(p,q)}).$$

From Assumption 1, it comes that under $\mathcal{H}_0$

$$\mathbb{E}[\widehat{R}^{\alpha}_{\tilde{Y}^{(p,q)}}(d^{(p,q)})] = 0. \tag{25}$$

To compute the covariance, we introduce the covariance matrix defined as

$$\mathbf{C} = \mathbb{E}[(\mathbf{R}-\mathbb{E}\{\mathbf{R}\})(\mathbf{R}-\mathbb{E}\{\mathbf{R}\})^H],$$

where the superscript ^{H} stands for transpose conjugate and

$$\mathbf{R} = [\widehat{R}^{\alpha_0}_{\tilde{Y}^{(p,q)}}(d^{(p,q)}), \widehat{R}^{\alpha_1}_{\tilde{Y}^{(p,q)}}(d^{(p,q)}), \ldots, \widehat{R}^{\alpha_{\mathrm{card}(\mathcal{A}_{(p,q)})-1}}_{\tilde{Y}^{(p,q)}}(d^{(p,q)})]^T.$$

If we now focus on each element $[\mathbf{C}]_{i,j} = \mathbb{E}[\widehat{R}^{\alpha_i}_{\tilde{Y}^{(p,q)}}(d^{(p,q)})(\widehat{R}^{\alpha_j}_{\tilde{Y}^{(p,q)}}(d^{(p,q)}))^*]$, we have

$$[\mathbf{C}]_{i,j} = \frac{1}{(M-d^{(p,q)})^2} \sum_{k_i,k_j=0}^{M-d^{(p,q)}-1} \mathbb{E}[\tilde{Y}_{k_i}(p)\tilde{Y}^*_{k_i+d^{(p,q)}}(q)\tilde{Y}^*_{k_j}(p)\tilde{Y}_{k_j+d^{(p,q)}}(q)]$$

$$\times e^{-i2\pi(k_i\alpha_i - k_j\alpha_j)}.$$

Thanks to Assumption 1, we get

$$\mathbb{E}[\tilde{Y}_{k_i}(p)\tilde{Y}^*_{k_i+d^{(p,q)}}(q)\tilde{Y}^*_{k_j}(p)\tilde{Y}_{k_j+d^{(p,q)}}(q)]$$
$$= \mathbb{E}[\tilde{Y}_{k_i}(p)\tilde{Y}^*_{k_j}(p)]\mathbb{E}[\tilde{Y}^*_{k_i+d^{(p,q)}}(q)\tilde{Y}_{k_j+d^{(p,q)}}(q)].$$

This term is different from zero only if k_i=k_j. Moreover, as shown in Eq. (10), $\tilde{Y}_k(n)$ is expressed as a ratio of two random variables. The variance estimator introduced in Eq. (11) being consistent, it converges almost surely to a constant denoted ν_n so that, thanks to the asymptotic theory developed in [49], $\tilde{Y}_k(n)$ converges in distribution to $Y(n)/\sqrt{\nu_n}$. Thus, for k_i=k_j and a time invariant

propagation channel

$$\mathbb{E}[\tilde{Y}_{k_i}(p)\tilde{Y}^*_{k_i+d^{(p,q)}}(q)\tilde{Y}^*_{k_j}(p)\tilde{Y}_{k_j+d^{(p,q)}}(q)] = \frac{\mathbb{E}[|Y_{k_i}(p)|^2]\mathbb{E}[|Y_{k_i}(q)|^2]}{\nu_p\nu_q} = 1$$

since $\nu_n = \mathbb{E}[|Y_k(n)|^2]$ and thanks to Assumption 1. Therefore, the asymptotic covariance is expressed as

$$[\mathbf{C}]_{i,j} = \frac{1}{(M-d^{(p,q)})^2}\sum_{k=0}^{M-d^{(p,q)}-1} e^{-i2\pi k(\alpha_i-\alpha_j)} = \frac{\sin(\pi(M-d^{(p,q)})(\alpha_i-\alpha_j))}{(M-d^{(p,q)})^2\sin(\pi(\alpha_i-\alpha_j))} e^{-i\pi(\alpha_i-\alpha_j)(M-d^{(p,q)}-1)}. \quad (26)$$

From Eq. (26) we can deduce that the correlation between $\widehat{R}^{\alpha_i}_{\tilde{Y}^{(p,q)}}(d^{(p,q)})$ and $\widehat{R}^{\alpha_j}_{\tilde{Y}^{(p,q)}}(d^{(p,q)})$ for $\alpha_i \neq \alpha_j$ is upper bounded by

$$|[\mathbf{C}]_{i,j}| \leq \frac{1}{(M-d^{(p,q)})^2\sin(\pi(\alpha_i-\alpha_j))} \leq \frac{1}{(M-d^{(p,q)})^2\sin(\pi/K)}$$

which implies that as long as $K \ll \pi(M-d^{(p,q)})^2$, the cyclic cross-correlation coefficients are asymptotically mutually independent. Thus, thanks to the central limit theorem and according to Eqs. (25) and (26)

$$\widehat{R}^{\alpha}_{\tilde{Y}^{(p,q)}}(d^{(p,q)})|\mathcal{H}_0 \overset{\mathcal{D}}{\mapsto} \mathcal{CN}\left(0, \frac{1}{M-d^{(p,q)}}\right),$$

where $\overset{\mathcal{D}}{\mapsto}$ indicates the convergence in distribution. The cyclic cross-correlation coefficients estimate being asymptotic uncorrelated Gaussian variables, it follows that $\tilde{Y}|\mathcal{H}_0$ can be expressed as a sum of weighted central chi-square variables. We now consider the following properties:

Property 5. *The characteristic function of a central chi-square variable X of ζ degree of freedom is written as $\psi_X(t) = (1-2it)^{-\zeta/2}$.*

Property 6. *Let $X_0, X_1, \ldots, X_{n-1}$ being mutually independent random variables of characteristic functions $\psi_{X_0}, \psi_{X_1}, \ldots, \psi_{X_{n-1}}$. Then, the characteristic function of $Y = \sum_{k=0}^{n-1} a_k X_k$ is defined as*

$$\psi_Y(t) = \prod_{k=0}^{n-1} \psi_{X_k}(a_k t).$$

Therefore, from Properties 5 and 6, we finally get

$$\psi_{J_{PIC}|\mathcal{H}_0}(t) = \prod_{(p,q)\in\xi}\left(1-\frac{it}{M-d^{(p,q)}}\right)^{-\mathrm{card}(\mathcal{A}_{(p,q)})}.$$

The inversion of this characteristic function using the results presented in [37] concludes the proof.

References

[1] F. Socheleau, S. Houcke, A. Aissa-El-Bey, P. Ciblat, OFDM system identification based on m-sequence signatures in cognitive radio context, in: IEEE Conference on Personal, Indoor and Mobile Radio Communications, 2008.
[2] F.-X. Socheleau, P. Ciblat, S. Houcke, OFDM system identification for cognitive radio based on pilot induced cyclostationarity, in: IEEE WCNC, 2009.
[3] U.S. FCC, Review of Spectrum Management Practices, 2002.
[4] U.S. FCC, Second Report and Order and Memorandum Opinion and Order, in the Matter of Unlicensed Operation in the TV Broadcast Bands Additional Spectrum for Unlicensed Devices Below 900 MHz and in the 3 GHz Band, 2008.
[5] J.M. Mitola III, Cognitive radio an integrated agent architecture for software defined radio, Ph.D. Thesis, KTH Royal Institute of Technology, Stockholm, Sweden, 2000.
[6] S. Haykin, Cognitive radio: brain-empowered wireless communications, IEEE Journal on Selected Areas in Communications 23 (2) (2005) 201–220.
[7] IEEE Dynamic Spectrum Access Networks Conference ⟨http://www.ieee-dyspan.org/⟩.
[8] M. Haddad, A. Hayar, M. Debbah, Spectral efficiency of cognitive radio systems, in: IEEE GLOBECOM, 2007.
[9] Software Defined Radio Forum ⟨http://www.sdrforum.org/⟩.
[10] J. McNair, F. Zhu, Vertical handoffs in fourth-generation multinetwork environments, IEEE Wireless Communications 11 (3) (2004).
[11] Z. Dai, R. Fracchia, J. Gosteau, P. Pellati, G. Vivier, Vertical handover criteria and algorithm in IEEE802.11 and 802.16 hybrid networks, in: IEEE International Conference on Communications, 2008.
[12] C. Stevenson, G. Chouinard, L. Zhongding, H. Wendong, S. Shellhammer, W. Caldwell, IEEE 802.22: the first cognitive radio wireless regional area network standard, IEEE Communications Magazine 47 (1) (2009).
[13] C. Cordeiro, K. Challapali, D. Birru, S. Shankar, IEEE 802.22: an introduction to the first wireless standard based on cognitive radios, Journal of Communications 1 (1) (2006) 38–47.
[14] S.V. Nagaraj, Entropy-based spectrum sensing in cognitive radio, Signal Processing 89 (32) (2009) 174–180.
[15] T. Yucek, Channel, spectrum, and waveform awareness in OFDM-based cognitive radio systems, Ph.D. Thesis, University of South Florida, 2007.
[16] M. Oner, F. Jondral, On the extraction of the channel allocation information in spectrum pooling systems, IEEE Journal on Selected Areas in Communications 25 (3) (2007).
[17] T. Yucek, H. Arslan, OFDM signal identification and transmission parameter estimation for cognitive radio applications, in: IEEE Global Telecommunications, , 2007, pp. 4056–4060.
[18] H. Li, Y. Bar-Ness, A. Abdi, O. Somekh, W. Su, OFDM modulation classification and parameters extraction, in: IEEE Conference on Cognitive Radio Oriented Wireless Networks and Communications, , 2006, pp. 1–6.
[19] H. Ishii, G.W. Wornell, OFDM blind parameter identification in cognitive radios, in: IEEE Conference on Personal, Indoor and Mobile Radio Communications, , 2005, pp. 700–705.
[20] A. Bouzegzi, P. Ciblat, P. Jallon, New algorithms for blind recognition of OFDM based systems, Signal Processing 90 (3) (2010) 900–913.
[21] N. Khambekar, L. Dong, V. Chaudhary, Utilizing OFDM guard interval for spectrum sensing, in: IEEE Wireless Communications and Networking Conference, , 2007, pp. 38–42.
[22] P. Sutton, K. Nolan, L. Doyle, Cyclostationary signatures in practical cognitive radio applications, IEEE Journal on Selected Areas in Communications 26 (1) (2008) 13–24.
[23] K. Maeda, A. Benjebbour, T. Asai, T. Furuno, T. Ohya, Recognition among OFDM-based systems utilizing cyclostationarity-inducing transmission, in: IEEE Symposium on New Frontiers in Dynamic Spectrum Access Networks, , 2007, pp. 516–523.
[24] Y. Shen, E. Martinez, Channel Estimation in OFDM Systems, Freescale Semiconductor, 2006.
[25] T. Schmidl, D. Cox, Robust frequency and timing synchronization for OFDM, IEEE Transactions on Communications 45 (12) (1997) 1613–1621.
[26] IEEE Std. 802.16, Part 16: Air Interface for Fixed and Mobile Broadband Wireless Access Systems, Amendment 2: Physical and Medium Access Control Layers for Combined Fixed and Mobile Operations in License Bands and Corrigendum 1, 2005.
[27] K. Wesolowski, On the PAPR minimization using selected mapping algorithm in pilot-assisted OFDM systems, in: European Wireless Conference, 2007.
[28] M.J.F.-G. Garca, O. Edfors, J.M. Pez-Borrallo, Peak power reduction for OFDM systems with orthogonal pilot sequences, IEEE Transactions on Wireless Communications 5 (1) (2006) 47–51.
[29] S. Ohno, G. Giannakis, Optimal training and redundant precoding for block transmissions with application to wireless OFDM, IEEE Transactions on Communications 50 (12) (2002) 2113–2123.
[30] E.D. Re, Software Radio: Technologies and Services, Springer, 2001.
[31] J.H. Reed, Software Radio: A Modern Approach to Radio Engineering, Prentice Hall Communications Engineering and Emerging Technologies Series, 2002.
[32] ETSI EN 300 744 V1.5.1, Digital Video Broadcasting (DVB); Framing structure, channel coding and modulation for digital terrestrial television, 2004.

Please cite this article as: F.-X. Socheleau, et al., Cognitive OFDM system detection using pilot tones second and third-order cyclostationarity, Signal Process. (2010), doi:10.1016/j.sigpro.2010.07.003

[33] W.A. Gardner, A. Napolitano, L. Paurac, Cyclostationarity: half a century of research, Signal Processing 86 (4) (2006) 639–697.
[34] IEEE Std. 802.16, Part 16: Air Interface for Fixed Broadband Wireless Access Systems, 2004.
[35] IEEE Std. 802.11a, Part 11: Wireless LAN Medium Access Control (MAC) and Physical Layer (PHY) Specifications High-speed Physical Layer in the 5 GHz Band, 1999.
[36] A.V. Dandawaté, G.B. Giannakis, Statistical tests for presence of cyclostationarity, IEEE Transactions on Signal Processing 42 (9) (1994) 2355–2369.
[37] A.C. Martinez, F.L. Blazquez, Distribution of a sum of weighted noncentral chi-square variables, Sociedad de Estadistica e Investigacion Operativa test 14 (02) (2005) 397–415.
[38] H. Minn, V.K. Bhargava, K.B. Letaief, A robust timing and frequency synchronization for OFDM systems, IEEE Transactions on Wireless Communications 2 (2003) 822–839.
[39] Y. Li, L.J. Cimini, Bounds on the interchannel interference of OFDM in time-varying impairments, IEEE Transactions on Communications 49 (3) (2001) 401–404.
[40] K.N. Le, Insights on ICI and its effects on performance of OFDM systems, Digital Signal Processing 18 (6) (2008) 876–884.
[41] J. van de Beek, M. Sandell, P. Borjesson, ML estimation of time and frequency offset in OFDM systems, IEEE Transactions on Signal Processing 49 (1997) 1800–1805.
[42] B. Park, E. Ko, H. Cheon, C. Kang, D. Hong, A blind OFDM synchronization algorithm based on cyclic correlation, in: IEEE Globecom Conference, vol. 5, 2001, pp. 3116–3119.
[43] M. Xiaoli, G. Giannakis, S. Barbarossa, Non-data-aided frequency-offset and channel estimation in OFDM and related block transmissions, in: IEEE ICC, 2001.
[44] J.A. Nelder, R. Mead, A Simplex Method for Function Minimization, Computer Journal 7 (1965) 308–313.
[45] M.J.D. Powell, An efficient method for finding the minimum of a function of several variables without calculating derivatives, Computer Journal 7 (1964) 155–162.
[46] W.H. Press, S.A. Teukolsky, W.T. Vetterling, S.P. Flannery, Numerical Recipies, The Art of Scientific Computing, third ed., Wiley, 2007.
[47] M. Upena, D. Dalal, Y.P. Kosta, WiMAX New Developments, IN-TECH, 2009 〈http://sciyo.com/books/show/title/wimax-new-developments〉.
[48] F.J. MacWilliams, N.J.A. Sloane, Pseudo-random sequences and arrays, in: IEEE Proceedings, vol. 64, 1976, pp. 1715–1729.
[49] P. Brockwell, R. Davis, Time Series: Theory and Analysis, Springer, 1991.

Please cite this article as: F.-X. Socheleau, et al., Cognitive OFDM system detection using pilot tones second and third-order cyclostationarity, Signal Process. (2010), doi:10.1016/j.sigpro.2010.07.003